JOURNAL OF APPLIED POLYMER SCIENCE VOL. 15, PP. 853-866 (1971)

# Fracture Toughness of Glass Fiber-Reinforced Acetal Polymer

G. F. HARDY, *Celanese Research Company, Summit, New Jersey 07901*

## Synopsis

The critical stress field intensity factor for crack propagation, $K_{Ic}$, was determined for a large number of glass fiber-reinforced acetal copolymer compositions and for the unfilled resin. The results were interpreted in terms of a model previously proposed for the tensile behavior of these materials. The $K_{Ic}$ could be regarded as a linear function of the contribution of the fiber reinforcement to the tensile strength, but was otherwise substantially independent of the amount and length of the fibers and the nature of the fiber finish. From this relationship it was estimated that the inherent flaw size of these materials was of the order of magnitude of the fiber length. The observed variation of $K_{Ic}$ with loading rate was also consistent with the model. The notched Izod impact strength of these same materials was shown to be roughly equivalent to $G_{Ic}$, the critical strain energy release rate, or fracture energy per unit area, which can be computed from $K_{Ic}$ by the methods of fracture mechanics. The behavior of these crack propagation parameters is consistent with the previous hypothesis that failure is initiated by loss of adhesion between the matrix and those fibers which lie transverse to the applied load.

## INTRODUCTION

Impact tests are customarily used in evaluating reinforced thermoplastics to assess their practical toughness.[1-3] The limitations of such tests are well known: since the mechanics of the test are not well understood, the results are not directly useful for design calculations and little information is usually obtained as to the way in which fracture resistance varies with temperature, strain rate, and stress concentration.[4-6]

The methods of fracture mechanics have been very useful in meeting similar difficulties encountered in the testing of metals.[7] The basic concept which is used is that the growth of a crack is controlled by the stress and strain fields near the crack tip. Once determined on an idealized test specimen, these critical conditions can be regarded as basic properties of the material. In principle, one can calculate from them the loads required to extend a crack in an object of any shape. Growth of the crack may be regarded as initiating from inherent flaws characteristic of the material or fabrication process. The effects of temperature, rate of loading, and environmental agents can be readily treated in this way.

In applying fracture mechanics to materials which crack before widespread yielding has occurred, it is customary and convenient to use two related approaches: (1) The stress field at the tip of the crack is characterized

by a parameter $K$, or (2) the elastic strain energy released by crack extension (and consumed by the cracking process) is represented by the quantity $G$. In what follows, the critical conditions for crack extension are $K_{Ic}$ and $G_{Ic}$, where the numerical subscript indicates an opening mode of crack extension, as distinct from in-plane or transverse shear.

This approach has already been used, with some success, in the study of fiber laminates,[8–10] glassy thermoplastics,[11–13] and adhesive joints,[14,15] but does not seem to have been applied to fiber-reinforced thermoplastics. Since a better understanding of the factors that control the performance of these materials is needed, the present study was undertaken. For a typical reinforced thermoplastic system, the critical conditions for crack propagation were determined as a function of composition. It will be shown that the resistance to crack propagation is rather simply related to conventional tensile properties and that this approach can be used to interpret the significance of the usual notched Izod impact data for these materials.

## EXPERIMENTAL

### Materials and Fabrication

The experiments were performed on injection-molded specimens of acetal copolymer resin reinforced with short, fully dispersed E-glass fibers. As described in a previous publication,[16] the ultimate strength and elongation of these materials can often be increased greatly by adding small amounts (usually 0.01–0.03 wt-%) of ammonium chloride.

TABLE I
Glass Fiber Surface Treatments[a]

| Type | Resin finish | Coupling agent |
|---|---|---|
| A | epoxy (partial cure) | glycidoxysilane |
| B | poly(vinyl acetate) | vinylsilane |
| C | poly(vinyl acetate | vinylsilane |
| D | poly(vinyl acetate) | chromium complex |
| E | poly(vinyl acetate) | vinylsilane + chromium complex |
| F | poly(vinyl acetate) | chromium complex |
| G | poly(ethylene oxide) | vinylsilane + aminosilane |
| H | none | none |

[a]According to manufacturers.

The acetal copolymer had a melt flow rate of 9.0 g/10 min at 190°C (ASTM D1238, condition E). The various types of glass fiber, usually supplied as $\frac{1}{4}$-in. chopped strand, are listed in Table I, together with available information as to the composition of the binders and coupling agents. The powdered polymer, dry blended with ammonium chloride, if used, was melted on a two-roll mill at about 190°C. The chopped glass fiber was added carefully, and the mixture was milled for about 5 min. The hot product was pressed flat, then ground into coarse chips for injection molding.

TABLE II
Test Results

| Glass fiber | | Tensile properties at break | | | | Notched Izod impact strength, ft-lb/in. of notch |
|---|---|---|---|---|---|---|
| Type[a] | wt-% | Strength, psi | Elongation, % | $\sigma_f$[b] psi | $K_{Ic}$,[c] psi-in.$^{1/2}$ | |
| A | 10 | 10,120 | 3.3 | 2,520 | 3930[d] | 0.66 |
| A | 10 | 11,940 | 4.0 | 3,870 | 3820 | 0.77 |
| A | 20 | 12,060 | 2.7 | 4,790 | 4010 | 0.70 |
| A | 20 | 14,060 | 3.7 | 6,060 | 4190 | 0.83 |
| B | 20 | 9,560 | 2.8 | 2,180 | 4020[d] | 0.72 |
| H | 20 | 8,790 | 5.4 | 490 | 3680[d] | 0.59 |
| A | 30 | 13,560 | 2.4 | 6,190 | 4110 | 0.77 |
| A | 30 | 16,300 | 3.4 | 8,370 | 4680 | 0.94 |
| G | 30 | 15,160 | 3.3 | 7,260 | 4570 | 1.09 |
| A | 40 | 14,100 | 2.2 | 6,560 | 4150 | 0.86 |
| A | 40 | 14,220 | 1.8 | 7,070 | 4020 | 0.98 |
| A | 40 | 16,760 | 3.0 | 9,010 | 4660 | 1.13 |
| A | 40 | 20,590 | 3.0 | 12,840 | 5300 | 1.25 |
| B | 40 | 10,600 | 1.6 | 3,750 | ... | 0.75 |
| B | 40 | 11,200 | 1.5 | 4,540 | 3660 | 0.77 |
| B | 40 | 11,420 | 1.7 | 4,420 | 3960 | 0.84 |
| B | 40 | 12,110 | 1.5 | 5,450 | 4020 | 0.78 |
| B | 40 | 15,960 | 2.5 | 8,290 | ... | 0.99 |
| B | 40 | 16,980 | 2.3 | 9,390 | 4870 | 0.93 |
| B | 40 | 18,300 | 3.6 | 10,530 | 4830 | 1.18 |
| B | 40 | 18,850 | 2.9 | 11,100 | 5260 | 1.23 |
| B | 40 | 19,300 | 4.0 | 11,520 | 5210 | 1.24 |
| B | 30/10[e] | 10,280 | 1.6 | 3,440 | ... | 0.73 |
| B | 30/10[e] | 14,100 | 2.3 | 6,510 | ... | 0.82 |
| B | 20/20[e] | 9,620 | 1.8 | 2,480 | ... | 0.71 |
| B | 20/20[e] | 12,220 | 2.2 | 4,680 | ... | 0.72 |
| B | 10/30[e] | 9,010 | 1.8 | 1,860 | ... | 0.66 |
| B | 10/30[e] | 10,520 | 2.4 | 2,890 | ... | 0.65 |
| C | 40 | 15,980 | 2.1 | 8,550 | 4510 | 0.92 |
| C | 40 | 16,950 | 2.3 | 9,370 | 4730 | 0.99 |
| C | 40 | 18,430 | 2.5 | 10,780 | 5290 | 1.30 |
| D | 40 | 15,290 | 1.8 | 8,130 | 4490 | 1.08 |
| D | 40 | 16,730 | 2.0 | 9,380 | 4870 | 1.18 |
| D | 40 | 19,460 | 2.7 | 11,750 | 5330 | 1.42 |
| E | 40 | 16,780 | 2.0 | 9,360 | 4800 | 0.94 |
| E | 40 | 17,460 | 2.3 | 9,880 | 4910 | 1.15 |
| E | 40 | 19,270 | 2.7 | 11,560 | 5060 | 1.25 |
| F | 40 | 15,980 | 1.9 | 8,680 | 4460 | 0.94 |
| F | 40 | 18,880 | 2.4 | 11,240 | 4950 | 1.08 |
| F | 40 | 20,370 | 3.1 | 12,610 | 5670 | 1.40 |
| H | 40 | 11,500 | 1.7 | 4,500 | 3910 | 0.82 |
| J[f] | 33 | 26,800 | 3.6 | 16,100 | 6060 | 1.56 |

[a] See Table I.

[b] Parallel fiber load at break, from eq. (2).

[c] Critical stress intensity factor, from eqs. (1).

[d] Net section breaking stress $>0.8\sigma_0$.

[e] Blend of long and short glass fibers, in amounts shown, as described by Hardy and Wagner.[16]

[f] Commercial glass-reinforced nylon composition.

ASTM Type I tensile bars, $\frac{1}{8}$ in. thick, were prepared from each composition, using a ram-type injection machine and a mold with moderately open gating at one end of the bar. Many of these bars had also been used in a previous investigation of tensile properties, in which pains were taken to keep the fiber orientation as constant as possible by controlling the injection molding conditions. Others were prepared at various times in a similar manner.

The final average glass fiber length in the molded bars ranged from about 0.2 to 0.7 mm, depending primarily on the amount of fiber present.

A commercial glass fiber-reinforced nylon 66 resin was also molded in the same way, for comparative purposes. This material contained 33 wt-% of randomly dispersed glass fibers, of about 0.4-mm average length after molding.

## Test Specimens

For the fracture toughness determination, the tensile bars were notched on both sides, at the middle of the gauge length section. Cuts about 0.06 in. deep and 0.006 in. wide were made in the narrow edges, using a screw slotting saw and a special jig to keep the slots in line with each other and perpendicular to the axis of the bar. Both cuts were then deepened to 0.075 ± 0.003 in. with a fresh single-edge razor blade held in a second jig. Due

TABLE III
Effect of Elongation Rate on $K_{Ic}$

| Glass fiber | | $K_{Ic}$, psi-in.$^{1/2}$ | |
|---|---|---|---|
| Type[a] | wt-% | 0.2 in./min | 20 in./min |
| — | 0 | (3000)[b] | 2840 |
| H | 40 | 3910 | 3820 |
| B | 40 | 3960 | 4000 |
| B | 40 | 4830 | 4810 |
| B | 40 | 4870 | 5130 |
| B | 40 | 5260 | 5590 |
| J[c] | 33 | 6060 | 6410 |

[a] See Table I.
[b] Estimated from data in Table IV.
[c] Commercial glass-reinforced nylon.

to elastic relaxation, the tips of the cracks thus formed were always much less than 0.001 in. in radius. After the bars had been broken as described below, the exact depth of the notch from which fracture started was determined with an optical comparator.

The notched bars, and normal tensile bars from the same lot, were broken in tension at a cross-head rate of 0.2 in./min in accordance with ASTM D638. Several groups of specimens were also tested at a cross-head rate of 20 in./min. using a Sanborn 150 short-response time load recorder.

Notched Izod specimens were cut from the central portion of the gauge length of tensile bars from each lot and tested in accordance with ASTM D256. The conditions of specimen preparation and testing were carefully standardized to ensure reproducible results. Since apparently minor changes in procedure can markedly change the Izod values obtained for materials of this type, the numbers obtained cannot be directly compared to other published data.

All the polyacetal specimens were conditioned for 48 hr at 23°C and 50% R.H. The nylon specimens were tested dry, as molded, after aging 48 hr in a closed container; they were exposed to the laboratory air as briefly as possible during preparation.

The results of these tests are summarized in Tables II and III.

## Computation and Validity of $K_{Ic}$

For each series of tests, the Irwin critical stress field intensity parameter $K_{Ic}$ was calculated by iteration between the following relations:[17]

$$K_{Ic} = \sigma_c a^{1/2}[1.98 + 0.36(2a/W) - 2.12(2a/W)^2 + 3.42(2a/W)^3] \quad (1a)$$

$$a = a_0 + \frac{K_{Ic}^2}{2\pi\sigma_0^2} \quad (1b)$$

where $\sigma_c$ is the measured breaking strength of the notched specimens, computed on the original cross section before notching; $W$ is the width of this cross section, $a_0$ is the notch depth, and the tensile strength of unnotched bars is $\sigma_0$. The results of this computation are given in Table II.

For a valid plane strain fracture toughness determination, several conditions must be met; essentially these are defined by the requirement that the critically loaded zone at the crack tip must be small relative to all specimen dimensions.[18] One proposed rule is that the net breaking stress across the notched section be no greater than $0.8\sigma_0$; all but three of the determinations (indicated in Table II) meet this test. The size of the specimens used meets the original recommendations of Srawley and Brown,[18] but not their later, much more severe restrictions on thickness.[17] An inspection of the data for metals whicb support these recommendations indicates that the maximum error in $K_{Ic}$ from this cause is unlikely to be greater than 5%–10%. (Specimens of inadequate size will tend to give an apparent $K_c$ which is too high.)

One reason for the restriction on minimum specimen size is to ensure a sudden onset of crack growth as the load increases. All of the specimens tested in the present series broke very suddenly at the maximum recorded load. In eqs. (1), $a_0$ is the crack length at the beginning of rapid growth, which was equal to the original notch depth in every case examined. Two methods were used to confirm this: notch tips were followed with a low-power telescope during loading, or a drop of ink was placed at the tip and the edge of the stain was later compared with the end of the razor-blade cut.

Equations (1) were derived for linear elastic, isotropic materials. While there was certainly some curvature in the stress–strain relations of these materials, it was not very great up to the notched break point, so linearity seems to be a reasonable approximation. The molded bars were not isotropic in their properties, but a consideration of probable flow patterns in the mold suggests that they were tested along principal directions of elastic symmetry. Wu[19] and Sih and co-workers[20] have shown that the same method will apply to orthotropic materials in that case.

### $K_{Ic}$ of the Resin Matrix

Similar measurements were performed on notched, injection-molded bars of the same polyacetal resin, without glass fibers. The results obtained at several cross-head speeds are summarized in Table IV. For the unfilled resin, the net section breaking stress of these bars was greater than $0.8\sigma_0$ at 0.2 in./min, but the restriction was met at higher cross-head speeds. On this basis, we may roughly estimate that the true $K_{Ic}$ for the resin matrix is around 3000 psi-in.$^{1/2}$ at 0.2 in./min.

TABLE IV
Test Results for Polyacetal Resin

| Cross-head speed, in./min | $K_{Ic}$, psi-in.$^{1/2}$ | $\sigma_c(\text{net})/\sigma_0$ |
|---|---|---|
| 0.02 | 3410 | 0.94 |
| 0.2 | 3420 | 0.89 |
| 2 | 3040 | 0.77 |
| 20 | 2840 | 0.69 |

## RESULTS

The values of $K_{Ic}$ and notched Izod impact strength for each composition of Table II were plotted against the corresponding tensile strength in Figure 1. (Note that the three points for $K_{Ic}$ of the filled polyacetal at the lowest tensile strengths are undoubtedly too high, as discussed above.) In both cases, the data for all the reinforced polyacetals lie on a single curve, regardless of the amount of fiber used, the resin finish and coupling agent, or the strengthening effect of any added ammonium chloride. The two points for glass-reinforced nylon lie well below these curves. The uncorrected $K_{Ic}$ of the polyacetal matrix at the same test speed lies on the curve defined by the reinforced specimens, but the notched Izod impact strength of the pure resin is approximately twice the value extrapolated from the other data.

The values listed in Table III indicate that a hundredfold increase in testing speed had little effect on the magnitude of $K_{Ic}$ for reinforced specimens. The observed differences are not much greater than the normal variation between repeat tests. There is, however, a trend toward a decrease in $K_{Ic}$ with test speed for low values of $K_{Ic}$ and an increase for high values.

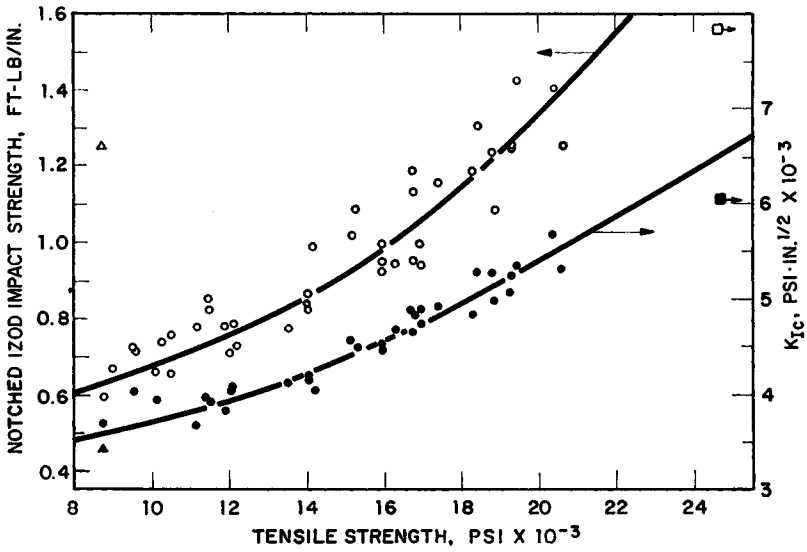


Fig. 1. Notched Izod impact strength (O) and $K_{Ic}$ (●) of the glass-reinforced polyacetal specimens, plotted against tensile strength. Also shown are the results of the same tests on unfilled polyacetal resin (△,▲) and a sample of glass-reinforced nylon 66 (□,■).

It will be shown below that these results are consistent with a mechanical model for the tensile behavior of reinforced thermoplastics, which has been previously proposed.[16] At this point, it should be pointed out that the crack propagation resistance of these materials, whether measured by $K_{Ic}$ or Izod impact strength, may be predicted quite accurately from the results of conventional tensile tests, using the empirical correlation of Figure 1.

## DISCUSSION

### Model for Tensile Behavior

It has previously been shown that the following simplified model accounts very well for the main features of the tensile stress–strain curve of these materials. The actual, more or less randomly dispersed fibers are assigned to two groups, considered to be parallel and transverse to the applied load. The parallel fibers bear a portion of the load, while the transverse fibers stiffen the matrix by strain concentration.

Up to the point at which fiber–matrix separation begins to occur, the tensile behavior is represented by

$$\sigma = \sigma_f + \sigma_m = \alpha\beta V_f E_f \epsilon + (1 - \alpha V_f)\sigma_{r,\gamma\epsilon} \qquad (2)$$

where $\sigma$ is the applied stress, $\sigma_f$ and $\sigma_m$ are the portions supported by the parallel fibers and by the combination of resin and transverse fibers, $\alpha$ is the fraction of the total fiber content assigned to parallel fibers, $\beta$ is an effi-

ciency factor for parallel fibers (a known function of the average fiber length), $V_f$ is the total volume fraction of fibers, $E_f$ is their Young's modulus, and $\epsilon$ is the overall specimen strain; $\sigma_{r,\gamma\epsilon}$ is the stress in unfilled matrix resin at a strain $\gamma\epsilon$, where the $\gamma$ factor accounts for strain concentration by the transverse fibers.

TABLE V
Experimental Stress–Strain Parameters for Injection Molded Specimens[a]

| Fiber content, wt-% | $\alpha$ | $\beta$ | $\gamma$ |
|---|---|---|---|
| 10 | 0.40 | 0.51 | 1.15 |
| 20 | 0.40 | 0.42 | 1.35 |
| 30 | 0.40 | 0.38 | 1.65 |
| 40 | 0.40 | 0.29–0.31 | 2.05 |
| 33[b] | 0.40 | 0.54 | 1.60 |

[a] From Hardy and Wagner.[16]
[b] Commercial glass fiber–nylon blend.

The values of the parameters $\alpha$, $\beta$, and $\gamma$ previously evaluated for compositions representative of those listed in Table II are summarized in Table V.

## Critical Stress Intensity $K_{Ic}$

For each test listed in Table II, the value of $\sigma_f$ was estimated, at the normal tensile strength, by using eq. (2). This was done by computing $\sigma_{r,\gamma\epsilon}$ from the strain at break, values of $\gamma$ from Table V, and the stress–strain curve of unfilled resin. Since $\sigma_{r,\gamma\epsilon}$ varies relatively slowly near the maximum strength, minor errors in the determination of $\epsilon$ and effects due to resin–fiber separation were probably not important.

In Figure 2, the value of $K_{Ic}$ for each composition has been plotted against $\sigma_f$. The points lie close to a straight line, which extrapolates to a $K_{Ic}$ of 3000 psi-in.$^{1/2}$ at zero $\sigma_f$. This value agrees very well with our conclusion (discussed above) as to the true $K_{Ic}$ of unfilled polyacetal resin. Only the three values of $K_{Ic}$ which were expected to be too high (see above) deviate greatly from this line. It is also worthy of note that the point for glass-reinforced nylon resin now lies on the same line.

In the earlier discussion of tensile strength, it was suggested that the evidence points to initiation of tensile failure by separation of the resin from the transverse fibers. In combination with the results just quoted, the following model is proposed for crack growth in these materials. Near the tip of the crack, resin pulls away from the transverse fibers, under the influence of the localized stress concentration, producing a region containing voids, or microcracks. These voids extend and join up under the combined influence of the tensile load and the resisting force of the parallel fibers which stitch together the flawed region. The growth process is thus equivalent to brittle crack propagation in unfilled resin, with the one difference that the

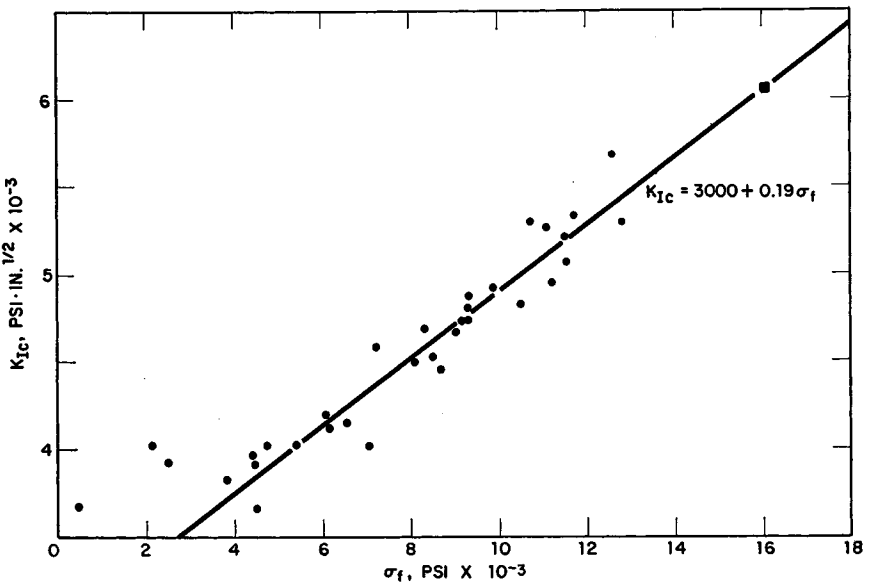


Fig. 2. $K_{Ic}$ for all specimens tested, plotted against $\sigma_f$, the contribution of the fibers to tensile strength. The symbols used are the same as those of Fig. 1. The regression line shown was fitted to all but the three dubious values of $K_{Ic}$ (see text).

compressive force of the parallel fibers must be overcome by an increased load.

We now use one of the outstanding advantages of the stress intensity approach to fracture resistance: the principle that the behavior of a crack subjected to several systems of forces can be predicted by summing the stress intensity factor $K$ computed separately for each set of forces.[21] For the specimen geometry used in these experiments,

$$K_{Ic} \cong 0.6\sigma_c, \tag{3}$$

and using eq. (2),

$$K_{Ic} \cong 0.6(\sigma_{c,f} + \sigma_{c,m}) = K_{Ic,m} + 0.6\sigma_{c,f} \tag{4}$$

The points in Figure 2 lie near the line

$$K_{Ic} = 3000 + 0.19\sigma_f. \tag{5}$$

So we have

$$\sigma_{c,f} \cong {}^1/_3\sigma_f$$

or, from eq. (2), the cracks in all these notched specimens began to propagate at a specimen strain about one third the breaking strain of a normal tensile specimen. The corresponding factor for other configurations can be deduced from known[21] relations of the general type of eq. (1).

Using this same approach, we can estimate the size of the inherent flaws, from which fracture of a normal, unnotched tensile bar begins. For small through-cracks in a large plate or sheet,

$$K_{Ic} = (\pi d/2)^{1/2}\sigma_c$$

where $d$ is the flaw size. This should not differ greatly from the desired expression for a small internal elliptical crack in a three-dimensional body.[21] If we take $\sigma_c$ equal to the normal tensile strength and go through the same reasoning as above,

$$d = 2 \times (0.19)^2/\pi = 2.3 \times 10^{-2} \text{ in.} = 0.6 \text{ mm.}$$

This quantity is of the order of magnitude of the length of a glass fiber, as we would expect if our proposed mechanism of failure is correct.

The effects of loading rate on $K_{Ic}$ (Table III) are also in at least qualitative agreement with the predictions of our model. As in eq. (4), $K_{Ic}$ may be broken down into two terms, of differing dependence on strain rate. The first term, whose effect will predominate for small $K_{Ic}$, is the critical stress intensity factor for pure resin; as the data in Table IV indicate, this decreases somewhat with increasing strain rate. The second term is proportional to $\sigma_f$ and will be most important at high $K_{Ic}$. The rate dependence of this term is primarily controlled by the factor $\beta$ in eq. (2). This may be expressed as[16]

$$\beta = 1 - \frac{\tanh N}{N}$$

$$N = (G_b)^{1/2} \times (\text{constant})$$

where $G_b$ is the shear modulus of the matrix, which increases with strain rate. For the magnitudes involved here, $\beta$, and thus the second term of $K_{Ic}$, increases somewhat with increasing strain rate. The trend of the data in Table III agrees with these predictions.

## Notched Izod Impact Strength

The fracture energy per unit area (strain energy release rate) can be computed from $K_{Ic}$ by using the relation[21]

$$G_{Ic} = K_{Ic}^2/E^* \tag{6}$$

where $G_{Ic}$ is the fracture energy. For an isotropic material in plane strain,

$$E^* = \frac{E}{1 - \nu^2}$$

where $E$ is Young's modulus and $\nu$ is Poisson's ratio of the material. For orthotropic materials, $E^*$ is a more complex function of the various moduli and Poisson's ratios. In the present case, in which a moderately oriented material is tested in its strongest direction, $E^*$ may be expected to be some-

what lower than the average slope of the stress–strain curve measured in the orientation direction.

The energy $G_{Ic}$ should correspond, at least approximately, to the fracture energy measured in a notched Izod impact test.[18,22] If the Izod value $I$ is expressed, as usual, in ft-lb/in. of notch, then

$$G_{Ic} \cong 30I$$

when the specimen dimensions are those recommended in ASTM D256. This relation involves several assumptions and approximations. The computation must, of course, be carried out for a strain rate equivalent to that of the Izod test. More fundamentally, as discussed by Srawley and Brown,[18] this relation assumes that the loss in pendulum energy can be equated with that consumed in forming cracked surface, and that the resistance to crack extension is constant during the propagation of the crack through the specimen. Both assumptions may well be open to question, but this approach should be at least qualitatively valid.

The preceding discussion predicts that the square root of the notched Izod impact strength should be approximately a linear function of $\sigma_f$. Neglecting rate effects, and using eq. (5), we have

$$I^{1/2} = (3000 + 0.19\sigma_f)/(30E^*)^{1/2}. \quad (7)$$

In Figure 3, the data of Table II have been plotted in this way. The relation predicted by eq. (7) is also shown, for three values of $E^*$. This simple

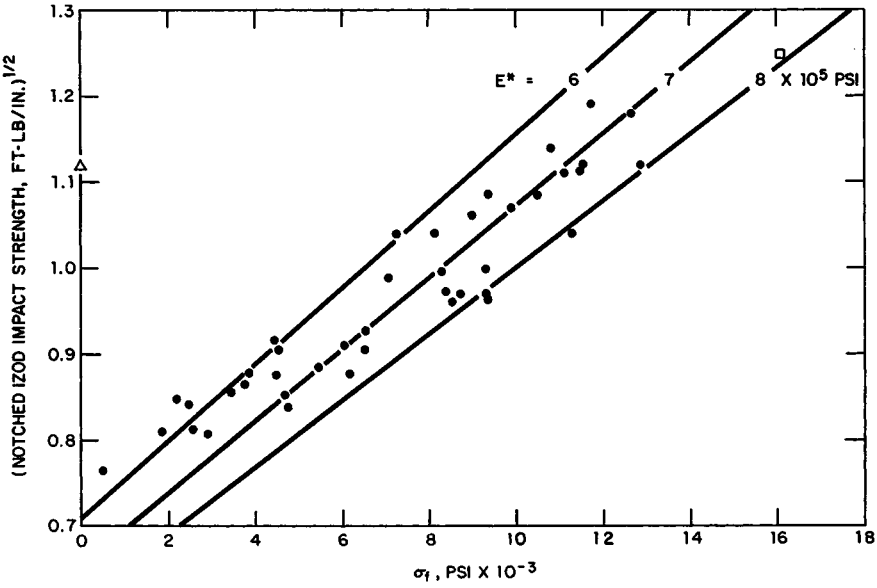


Fig. 3. The square root of notched Izod impact strength for all specimens, plotted against $\sigma_f$. Symbols as in Fig. 1. The lines represent eq. (7) for three values of the modulus $E^*$.

approach seems to agree fairly well with the observed behavior, and the resulting values of $E^*$ seem quite reasonable. It should be remembered that $E^*$ is the average slope of the entire stress–strain curve corrected by a factor not much greater than unity, and not the initial modulus, which is considerably higher.

It has been reported that, in some circumstances, slippage of fiber ends within the matrix can make a major contribution to the fracture energy.[9,10] In that case, as the matrix–fiber adhesion is increased, the energy of fracture will reach a maximum and begin to fall off before the condition of maximum tensile strength is attained. No indication of such an effect was seen in the present work, in which the energy rose monotonically with tensile strength. Slippage always occurred in preference to fiber breakage during failure; the fracture surfaces were covered with protruding fiber ends which were about half as long as the fibers themselves. This is because the fibers were generally too short to develop the maximum possible tensile stress.[16] If similar compositions could be prepared containing much longer fibers, the predicted energy effects might be observed.

At zero $\sigma_f$, the extrapolated notched Izod value is around 0.6 ft-lb/in. for the glass-filled materials, compared with about 1.25 ft-lb/in. for the pure resin. On the other hand, it was shown above that $K_{Ic}$ for these same compositions extrapolates to a value very close to that found for unfilled resin. This difference is undoubtedly due to the larger root radius of the notch specified for the conventional Izod test (0.010 in.) which may be insufficient to completely suppress gross yielding of the pure resin, even at the high test speed used. For two types of acetal copolymer, Williams and co-workers[23] obtained values of $G_{Ic}$ corresponding to notched Izod impact strengths of 0.3–0.7 when the specimens were sharply notched with a razor blade. It is also worth noting that a notched Izod impact strength of about 0.6 ft-lb/in. is obtained when gross yielding of the unfilled polyacetal is suppressed by testing at sufficiently low temperatures (−40°C or lower).

### Glass Fiber-Reinforced Nylon

In Figures 2 and 3, the points for dry glass-filled nylon 66 lie very close to the correlation established for the polyacetal compositions. This suggests that the $K_{Ic}$ and $G_{Ic}$ of the unfilled nylon resin are quite similar to the values for the polyacetal used, since the comparison on the basis of $\sigma_f$ should eliminate any differences due to the glass fiber. This conclusion is also in agreement with the data of Williams and co-workers for nylon 66.[23]

## CONCLUSIONS

The fracture resistance of the glass fiber-reinforced compositions studied seems to be wholly consistent with the model previously proposed for their tensile behavior. In particular, the critical stress intensity for crack propagation $K_{Ic}$ and the notched Izod impact strength $I$ are found to be linear

functions of $\sigma_f$ and $\sigma_f^2$, where $\sigma_f$ is the contribution to the tensile strength of that portion of the fibers which acts parallel to the applied load. This supplies a means of deriving these quantities from tensile test data, or estimating them approximately on the basis of the fiber length and orientation distribution.

As a corollary, it is seen that transversely oriented fibers, or other small rigid particles with no great extension in the direction of loading, will not be expected to make a significant contribution to fracture resistance, no matter how well bonded to the matrix. Since such a filler will tend to repress gross yielding, the crack propagation resistance will be considerably lower than that of the pure resin under transitional conditions, such as those of the notched Izod test at room temperature.

This approach is suggested to apply only to materials in which the fibers can be regarded as being well dispersed in the matrix. Compositions containing clumps of long fibers are often found to possess a rather high notched impact strength, together with a tensile strength which is not much greater than that of the unfilled resin. In this case, an appropriate model must consider the behavior of the fiber-rich regions separately from that of the bulk of the material. Such a treatment has not been attempted, but it seems likely that it could be carried out along much the same lines as the present argument.

The notched Izod test is seen to be a useful and valid measurement of one characteristic of glass-reinforced thermoplastics; namely, the resistance to enlargment of a preexisting flaw. It cannot, however, shed much light on the behavior of an unflawed specimen. For this, "practical" impact testing is required, in the absence of a reliable model for the initial failure process.

## References

1. L. Lee, *Polym. Eng. Sci.*, **9**, 213 (1969).
2. J. E. Theberge and N. T. Hall, *Mod. Plastics*, **46**, No. 7, 114 (1969).
3. H. S. Loveless and D. E. McWilliams, *Polym. Eng. Sci.*, **10**, 139 (1970).
4. M. N. Riddell and J. L. O'Toole, *Mod. Plastics*, **45**, No. 9, 150 (1968).
5. R. H. Shoulberg and J. J. Gouza, *SPE J.*, **23**, No. 12, 32 (1967).
6. P. I. Vincent, *Plastics Inst. Trans.*, **30**, 157 (1962).
7. G. R. Irwin, J. A. Kies and H. L. Smith, *ASTM Proc.* **58**, 640 (1958).
8. H. T. Corten, in *Fundamental Aspects of Fiber Reinforced Plastic Composites*, R. T. Schwartz and H. S. Schwartz, Eds., Interscience, New York, 1968, pp. 89–107.
9. J. O. Outwater and M. C. Murphy, paper presented at 24th Annual Meeting of the Reinforced Plastics/Composites Division of SPI, Washington, D.C., February 1969.
10. A. S. Tetelman, in *Composite Materials: Testing and Design, ASTM STP* **460**, 1969, pp. 473–502.
11. J. P. Berry, *J. Polym. Sci. A*, **1**, 993 (1963).
12. L. J. Broutman and F. J. McGarry, *J. Appl. Polym. Sci.*, **9**, 609 (1965).
13. P. L. Key, Y. Katz, and E. R. Parker, UCRL-17911, University of California, Lawrence Radiation Laboratory, February 1968.
14. M. L. Williams, *J. Appl. Polym. Sci.*, **13**, 29 (1969).
15. E. J. Ripling, S. Mostovoy and R. L. Patrick, in *Adhesion, ASTM STP* **360**, 1964, pp. 5–19.
16. G. F. Hardy and H. L. Wagner, *J. Appl. Polym. Sci.*, **13**, 961 (1969).

17. W. F. Brown and J. E. Srawley, *Plane Strain Crack Toughness Testing of High Strength Metallic Materials, ASTM STP* **410**, 1966.

18. J. E. Srawley and W. F. Brown, in *Fracture Toughness Testing and its Applications, ASTM STP* 381, 1965, pp. 133–196.

19. E. M. Wu, *J. Appl. Mech.*, **34**, 967 (1967).

20. G. C. Sih, P. C. Paris, and G. R. Irwin, *Int. J. Fract. Mech.*, **1**, 189 (1965).

21. P. C. Paris and G. C. Sih, in *Fracture Toughness Testing and its Applications, ASTM STP* 381, 1965, pp. 30–81.

22. B. Harris and E. M. de Ferran, *J. Mater. Sci.*, **4**, 1023 (1969).

23. J. G. Williams, J. C. Radon, and C. E. Turner, *Polym. Eng. Sci.*, **8**, 130 (1968).

Received October 22, 1970
Revised December 30, 1970